Determination of Jc and n-value of HTS Pellets by Measurement and Simulation of Magnetic Field Penetration

Bruno Douine, Charles-Henri Bonnard, Frédéric Sirois, Kévin Berger, Abelin Kameni Ntichi, Jean Lévêque

Determination of J_C and *n*-value of HTS Pellets by Measurement and Simulation of Magnetic Field Penetration

Bruno Douine, Charles Henri Bonnard, Frédéric Sirois, *Senior Member, IEEE*, Kevin Berger, Abelin Kameni, Jean Lévêque

***Abstract*—The complete penetration magnetic field B_P is a feature of superconducting sample submitted to an applied magnetic field. It is very important to know it for applications like electrical motor or levitation. The electric *E-J* characteristics of HTS bulk is generally described by a power law. The main purpose of this paper is to investigate the influence of the n-value and applied magnetic field rise rate V_b on the B_P of a HTS cylindrical pellet. The numerical results presented come from the resolution of a non linear diffusion problem with a commercial software. In this study, cylindrical HTS pellets are submitted to an axial applied magnetic field. With the help of these simulations a linear relationship between B_P, V_b and *n*-value has been found. A comparison between measurements and simulations is done for magnetization of cylindrical bulk superconducting samples. This comparison allows to determine the critical current density J_C and the n value of the power law $E(J) = E_C(J/J_C)^n$. The experiment is based on direct measurement of local magnetic field in the gap between two bulk HTS pellets. The field penetration measurements has been carried out on HTS pellets at 77 K by applying increasing magnetic fields with a quasi constant sweep rate for axial direction of the applied magnetic field. Two values of complete penetration magnetic field B_P have been measured at two different rise rates V_b. The *n*-value of the real HTS pellet has been deduced.**

***Index Terms*— Superconductor, magnetic field diffusion, critical current density**

1. INTRODUCTION

Studying bulk superconductor magnetization is essential for devising electrical motors or magnetic levitation systems. The recent developments in the processing of melt-textured high temperature superconductor (HTS) bulks with high critical current density make this form of the HTS material particularly promising for the above-mentioned applications [1]-[9].

Several authors have studied the magnetization of superconducting pellets [10]-[14]. For low temperature superconductors (LTS) or HTS materials used at low temperatures, the magnetization can be calculated from the critical state model (CSM) [15] because in this case CSM represents well the relationship between electric field *E* and current density *J*. Since in the CSM *J* can only take well defined values such as 0 or J_C (critical current density) that do not depend on the rate of variation of the externally applied field, it is possible to obtain analytical results for the magnetization of simple geometrical shapes, in particular cylinders [11], [12]. Inversely, because of this simple relationship, J_C can be determined by magnetization experiments, assuming that the CSM applies over the whole range of analysis [13]-[14], [16].

In the case of HTS used at "high temperatures" (typically above 50-60 K), a power law model (PLM) better represents the *E(J)* characteristic of the materials than the CSM model [17]-[20]. The PLM is typically written as:

$$E = E_C\left(\frac{J}{J_C}\right)^n = \frac{E_C}{J_C}\cdot\left(\frac{J}{J_C}\right)^{n-1} J \qquad (1)$$

The calculation of the magnetization of superconducting samples assuming a PLM requires numerical simulations, except in the case of infinite sheets [17], [18]. The determination of the J_C and *n* parameters defining the PLM for a given sample is not simple either. In the case of samples with a pellet-shape, the PLM parameters can be determined using ac susceptibility measurements [21], [22]. However, this approach leads to an indirect and complex relationship of the susceptibility with J_C and *n*. A simpler method would be desirable.

This paper presents an attempt to provide such a simpler method, by studying the influence of the n-value and the applied magnetic field rising rate V_b on the complete penetration magnetic field B_P of a cylindrical HTS pellet submitted to an uniform axial applied magnetic field $B_a(t)$ (Fig. 1). At the center of the pellet, the magnetic field $B_0(t)$ starts to rise after some time delay T_P, related to the moment at which B_a reaches B_P (Fig. 2). For cylinders, and assuming the Bean model applies [15], an analytic expression for the complete penetration field, named B_{PB}, can be obtained, i.e. [23]

$$B_{PB} = \frac{\mu_0 J_C . L}{4} . ln\left(\frac{\sqrt{R^2 + \left(\frac{L}{2}\right)^2} + R}{\sqrt{R^2 + \left(\frac{L}{2}\right)^2} - R}\right) \qquad (2)$$

where *L* is the length of cylinder and *R* is its radius. This formula is equivalent to similar formulas derived by other authors [24]-[27].

Manuscript received July 19, 2014.

B. Douine, C.H. Bonnard J. Lévêque and K. Berger, are with University of Lorraine, Groupe de Recherche en Electrotechnique et Electronique de Nancy, 54506 Vandoeuvre, France (e-mail: bruno.douine@univ-lorraine.fr, ch.bonnard.perso@gmail.com, jean.leveque@univ-lorraine.fr, kevin.berger@univ-lorraine.fr).

F. Sirois is with Ecole Polytechnique of Montreal, Montreal, QC H3C3A7, Canada (e-mail : f.sirois@polymtl.ca)

A. Kameni is with Group of Electrical Engineering of Paris (GeePS), Gif-sur-Yvette, France (e-mail: abelin.kameni@supelec.fr)

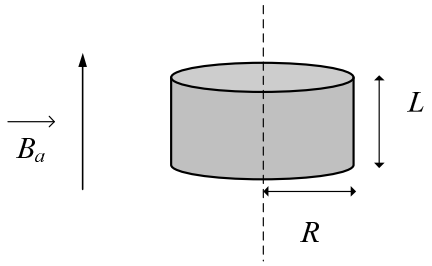

Fig. 1. Cylindrical bulk superconducting pellet submitted to a uniform axial magnetic field.

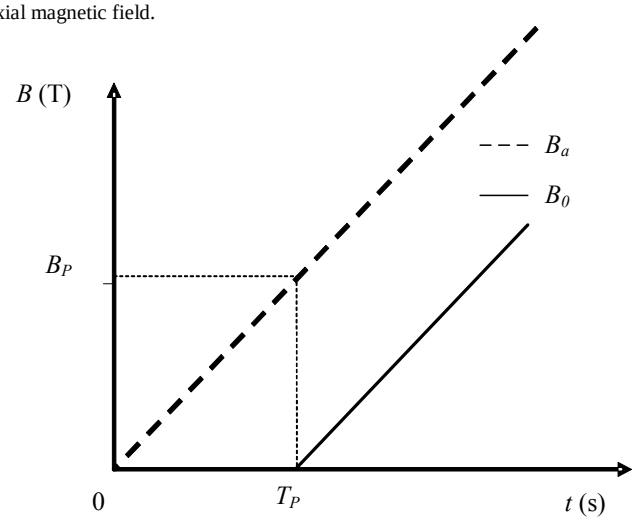

Fig. 2. Linearly growing applied magnetic field (B_a) and theoretical magnetic field (B_0) at the center of the pellet versus time (t).

From the above study, a method to determine the PLM parameters (J_C and n) of a cylindrical sample from experimental measurements is proposed. For a given J_C value, the use of the PLM implies that B_P is a function of the rising rate of the applied field (V_b) and the n value [13]. It is shown in the paper that a given n value generates a single $B_P(V_b)$ curve. Numerical simulations allowed us to determine an empirical $B_P(V_b)$ relationship, which in turns allowed us to determine n by comparing the measured and simulated $B_P(V_b)$ curves. It turns out that these $B_P(V_b)$ allow us to relate J_C and n with the experiments in a much simpler way than ac susceptibility measurements, mainly because the magnetic field is measured directly instead of being calculated by indirect means.

This paper is organized as follows. Firstly the computational approach is described. Secondly the influence of n and V_b on B_p is analyzed through numerical simulations. Thirdly, we propose an experiment that allows measuring the quantities of interest in conditions that are very similar to the simulations, and we discuss the experimental results. Finally, we summarize our new experimental method for determining the n-value of the PLM .

2. Numerical model

In order to observe the current and magnetic field distributions in the superconducting material, we developed a finite model of a typical pellet such as that illustrated in Fig. 1. The model was developed in the COMSOL multi-physics environment. In all simulations considered in this paper, the externally applied field was oriented along the central axis of the pellet (c-axis), and all results such as those shown in Fig. 2 represent the field component that is perpendicular to the flat faces of the pellet.

The field profiles can be computed using Faraday's law, Ampere's theorem and constitutive laws of superconducting material usually used for numerical simulation [28], [29]:

$$\nabla\times\vec{E} = -\frac{\partial\vec{B}}{\partial t} \tag{3}$$

$$\nabla\times\vec{H} = \vec{J} \tag{4}$$

$$E = \rho(J).J \text{ with } \rho(J) = \frac{E_C}{J_C}\left(\frac{|J|}{J_C}\right)^{n-1} \tag{5}$$

$$B = \mu_0 H \tag{6}$$

In order to speed-up convergence of the numerical problem, a small value ρ_0 equal to 1e-3*E_C/J_C was added to $\rho(J)$ [29]. Cartesian coordinates were used, and the axial component corresponded to the z-axis. The quantities E and J therefore have no axial component, but B has all three components in the 3-D case, i.e.

$$E = \begin{pmatrix} E_x \\ E_y \\ 0 \end{pmatrix} \quad J = \begin{pmatrix} J_x \\ J_y \\ 0 \end{pmatrix} \quad B = \begin{pmatrix} B_x = \mu_0 H_x \\ B_y = \mu_0 H_y \\ B_z = \mu_0 H_z \end{pmatrix}$$

Maxwell's equations (equ. 1 and 2) are written in a way that they only depend on H_x, H_y, H_z. Therefore a H-formulation is chosen, such as proposed in [30].

The superconductor is modeled using a nonlinear resistivity deduced from the PLM (1). Thus, in the general case, the resistivity depends on the current density J, as well as the temperature T. We apply boundary conditions on a surrounding cylinder whose diameter and height are respectively 10 times and 20 times the size of the pellet. Those large distances between the pellet and the boundaries allow us to impose Dirichlet conditions everywhere, i.e. $B_z(t) = B_a(t) = \mu_0.H_z(t)$ on all boundaries.

3. Influence of rise rate, n-value on B_P

In order to study numerically the influence of V_b on B_P, we performed simulations involving one pellet submitted to different V_b. For all simulations the applied magnetic field $B_a(t)$ was a linearly increasing field, as shown in Fig. 1. The pellet had a radius R of 1 cm and a thickness L of 1 cm, which corresponds to the pellets used in the experimental part of this work. The value of J_C chosen was 100 A/mm², which is a realistic value for HTS bulks at 77 K.

As shown in a previous article of ours [13], thermal effects can be neglected in our study (the rising rates of the field V_b are not high enough to result in significant heating). Nevertheless, for the highest rising rates considered here, the heat generated in the bulk is not so negligible, but we can still determine B_P just at the beginning of the ramp $B_0(t)$

at $t=T_P$. Therefore, for $0 < t < T_P$, the temperature rise in the superconducting pellet is limited to 1-2 K. As a result, the impact of the temperature on J_C remains weak during the magnetic field penetration phase.

A. *Distribution of current density as a function of V_b*

The value of the rising rate V_b changes the distribution of magnetic field and current density due to the *E(J)* power law characteristics used in the simulations instead of the Bean model [20]. To confirm this, several simulations have been performed with several values of V_b. The *n*-value chosen for the power-law model was 15, which is a likely n-value for HTS bulks. Fig. 3 presents the distributions of J/J_C in the pellets for V_b values of 0.1 T/s, 10 T/s and 1000 T/s, respectively, for the same value of B_a. These distributions show that with higher V_b, we observe lower penetration of magnetic field and current density, as expected from classical electrodynamics: higher variation of magnetic induction results in higher electric field, which translates in Fig. 3 to higher values of J/J_C. For high values of V_b (for example 100 T/s) J reaches almost $2*J_C$ (Fig. 3c).

B. *Influence of V_b and n on B_P*

As explained in the introduction and in Fig. 2, B_P is defined when $B_0(t)$ starts to rise at T_P. Therefore, in order to determine B_P from the simulations, the rise time T_P is identified and B_P is deduced. Fig. 4 shows the magnetic induction B_0 at the centre of the pellet for five different values of V_b ranging from 0.01 T/ to 1000 T/s, still with a n-value of 15. In order to allow comparisons between different rising rates on one figure, the magnetic field is represented versus $t*V_b$. Fig. 4 shows that a higher V_b leads to larger values of T_P and B_P, for the same reason as above.

From the $B_0(t*V_b)$ curves, the $B_P(V_b)$ curve can be deduced, as shown in Fig. 5 for n-values of 15 and 30, respectively. The figure also shows that B_{PB} is independent of V_b in the case of the Bean model.

In Fig. 4 and 5, we clearly see that both B_P and T_P increase with V_b. There is a nearly linear relationship between B_P and $\ln(V_b)$. Also, for values of V_b in the range of 0.1 T/s, B_P is equal to B_{PB} for all n-values. This is because J is approximately equal to J_C for this value of V_b. we will refer to this typical value of V_b as V_{b0}, corresponding to the rising rate V_b at which B_P is practically independent of the n-value. Fig. 5 shows also that for very low V_b (0.01 T/s) $B_P < B_{PB}$ because J is below J_C. In this case the penetration of current density is much larger than in the case of high V_b.

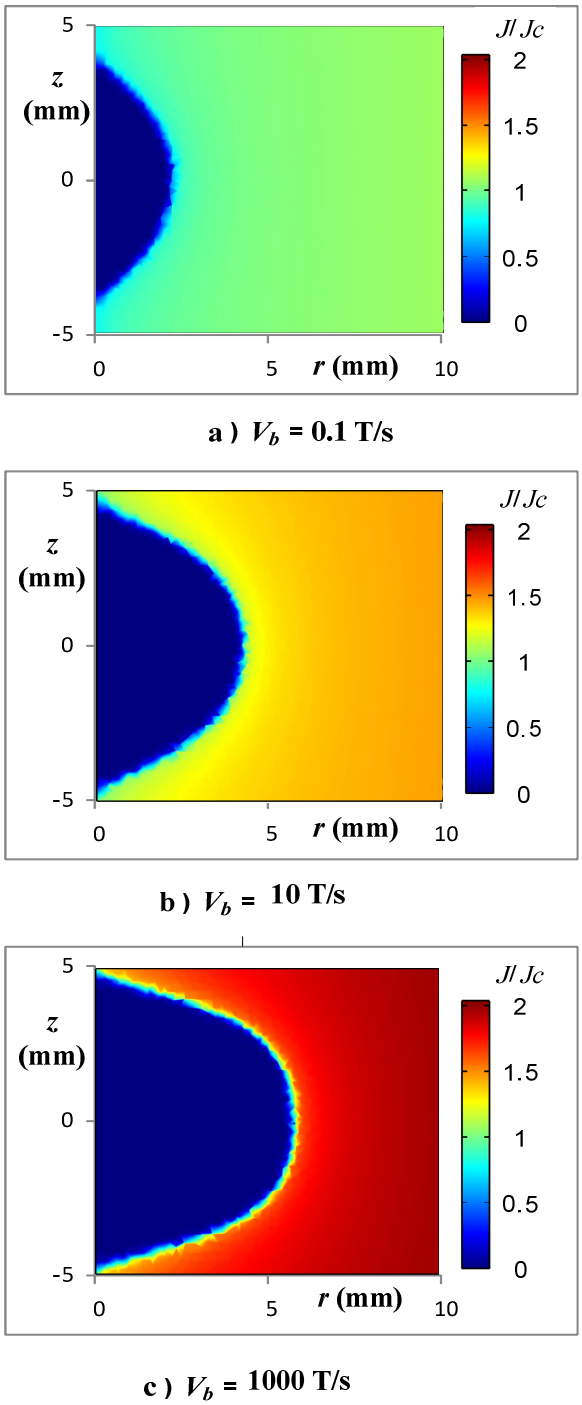

Fig. 3. J/J_C distributions in the pellet for different rising rates of the applied magnetic field for the same value of B_a

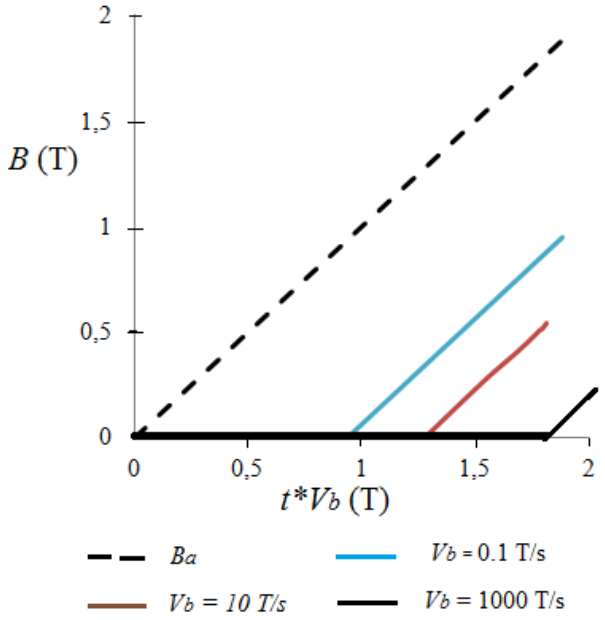

Fig. 4. Applied magnetic field and magnetic field at the center of the pellet for different rising rates V_b and n = 15.

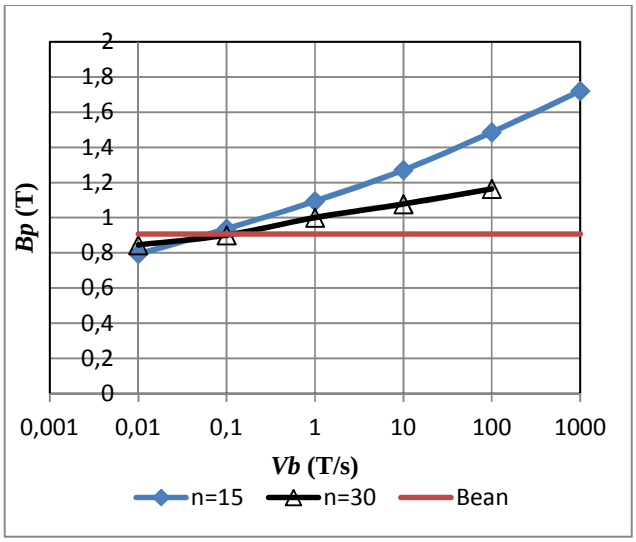

Fig. 5. B_P versus V_b for two different n-values (15 and 30) and B_{PB} (brown line) calculated from Bean model.

Fig. 6 shows B_a(t) and B_0(t) for different n-values and V_b = 100 T/s. This high value of V_b was chosen because the influence of n is very high in this case (see Fig. 5). Indeed, a higher n-value results in smaller T_P *and* B_P. This result is consistent with results in Fig.5.

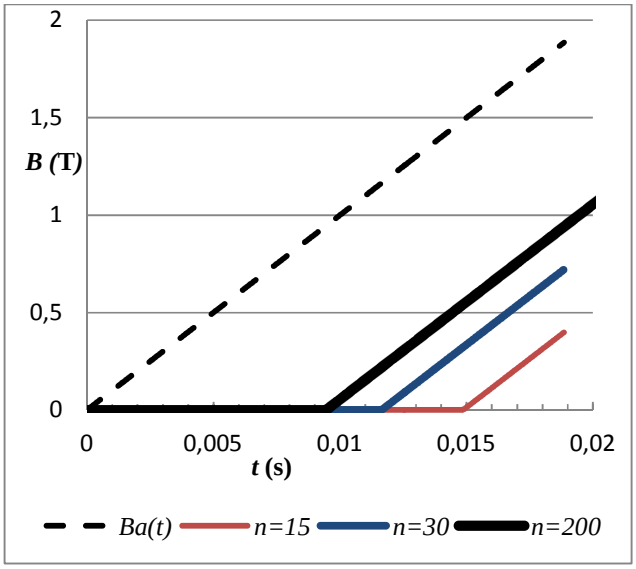

Fig. 6. Applied magnetic field B_a(t) and and magnetic field at the center of the pellet B_0(t) for different n-values and V_b=100T/s .

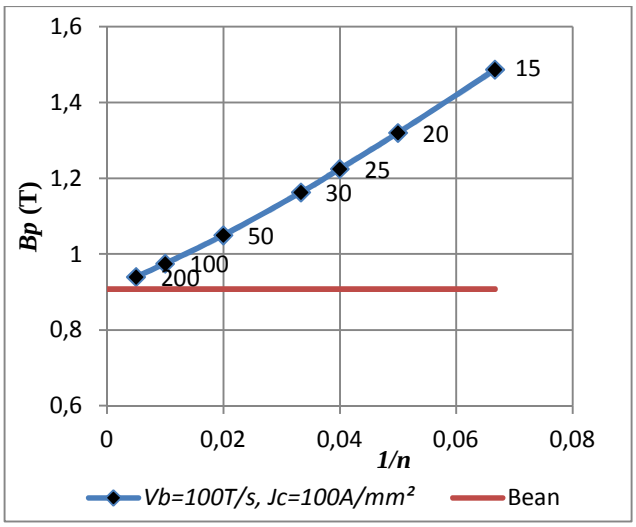

Fig. 7. B_P versus 1/n for different values of V_b and B_{PB}.

From these curves of B_0(t), we can trace B_P(1/n), as shown in Fig. 7 (V_b = 100 T/s and J_C = 100 A/mm²). In this case, B_{PB} equals corresponding to 0.91 T is also represented (brown line). We clearly observe that B_P increases linearly with 1/n. For a value of 1/n approaching zero, B_P tends to B_{PB}. This is because J is around J_C for high n-values, as in the case of the Bean model.

C. *Relationship between B_P and materials parameters*

As shown above, there is a nearly linear relationship between B_P and V_b and between B_P and 1/n.

Firstly it is important to note that B_P is equal to B_{PB} in two cases, i.e. at V_{b0} and also when 1/n is approaching zero. We can thus write:

$$B_P(V_{b0}) = B_P(n \to \infty) = B_{PB} \quad (7)$$

All geometric parameters, R and L, are included in B_{PB}. The value of J_C is also included in B_{PB}. So B_P depends on B_{PB}, V_b and the n-value. This is verified by simulation for realistic pellet dimensions and J_C values. To be consistent with (7), we choose to identify a linear relationship between B_P, B_{PB}, the n-value and $\ln(V_b)$ as:

$$B_P = B_{PB}\left(1+\frac{f(\ln V_b)}{n}\right) \quad (8)$$

So the function $f(\ln V_b)$ is equal to:

$$f(\ln V_b) = \frac{(B_P - B_{PB}).n}{B_{PB}}. \quad (9)$$

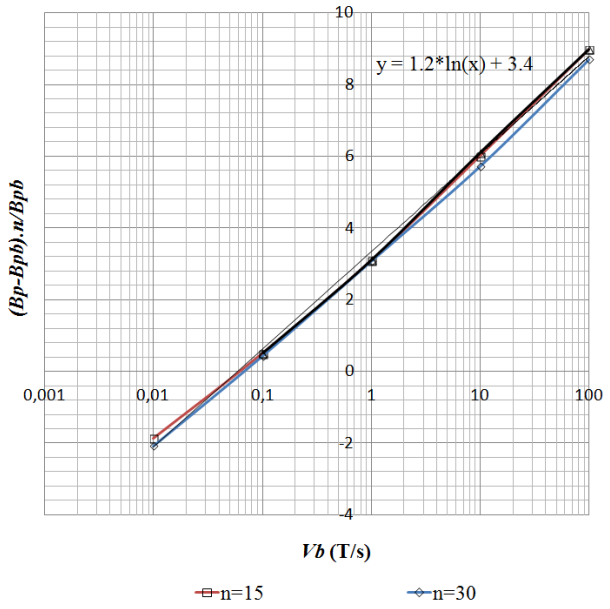

Fig. 8. f(ln Vb) =(B_P – B_{PB}).n/B_{PB} versus V_b for n = 15 and 30.

Fig. 8 represents $f(\ln V_b)$ versus $\ln V_b$ for two n-values, 15 and 30. The parameters of the linear function $f(\ln V_b)$ can be deduced from this figure based on the following explicit form:

$$B_P = B_{PB}\left(1+\frac{\alpha \ln V_b + \beta}{n}\right) \quad (10)$$

In this particular case $\alpha = 1.2$ and $\beta = 3.4$. The influence of geometric parameters R and L should be study in future work to give generality to the formula (10).

Therefore, this simulation study allowed us deducing an interesting relationship (10) between B_P, V_b and n. This relationship will prove to be useful experimentally for determining the n-value of a pellet submitted to different rising rates V_b of the external field.

4. Experimental setup, samples and results

Some authors already used Hall probes to determine magnetic field distribution in superconducting sample [31]-[33]. In order to use the results derived above by simulations, one need to measure the complete penetration magnetic field B_P in pellets. The main idea of our method is to separate the studied pellet in two pellets to allow deducing B_P from measurement of the complete penetration magnetic field B_{PM} between these two pellets. The magnetic field is detected with an axial Hall probe placed on the central axis of two HTS pellets (Fig. 9). To allow comparison between theoretical calculated B_P and measured B_{PM}, the thickness e of the Hall probe has to be taken into account. In our case, a thickness of 1.0 mm was taken (worst case scenario). In part 5 the influence of thickness e is numerically studied and especially for e = 1 mm to deduce B_P from B_{PM}

The cylindrical HTS pellets used in this experiment were YBCO pellets of 10 mm of radius (R) and 0.5 cm of thickness (L/2). In the simulation, the thickness of the corresponding pellet was taken as L, i.e. the sum of the two half-pellets.

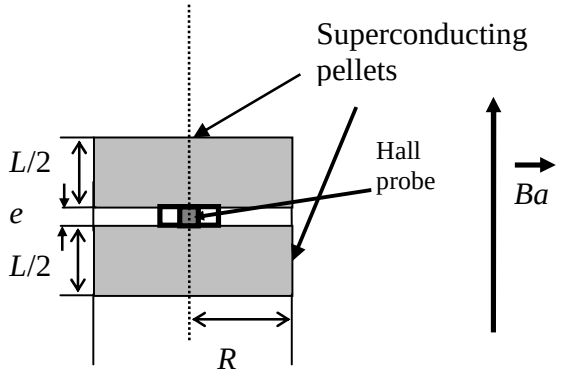

Fig. 9. Hall probe location between two HTS pellets

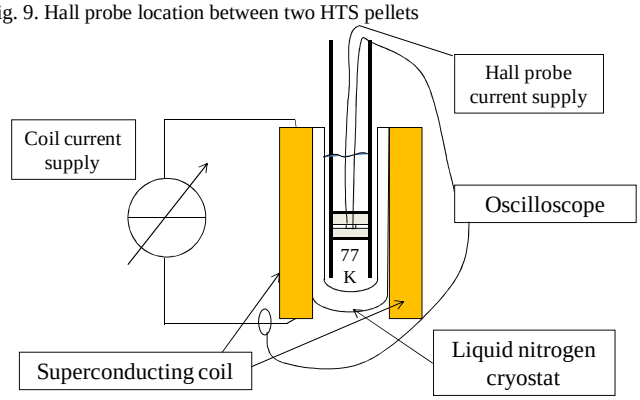

Fig. 10. Experimental set up using a superconducting coil for applying slowly varying external fields to YBCO pellets used in this experiment

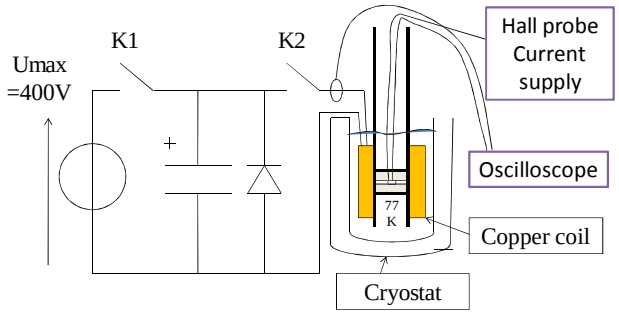

Fig. 11. Pulsed experimental set up used for higher rising field rates (using a copper coil).

In order to study experimentally the influence of rising rate on the magnetic field penetration, the measurement of B_{PM} has been done for two different rising rates. We used two different experimental setups for generating the low and high rising rates. For the low rising rate, a superconducting coil supplied by a current source was used (Fig. 10). For the high rising rate, the superconducting coil could not be used because the losses that would be generated would quench it. Therefore, a pulsed field magnetization process [13] based on a copper coil was used (Fig. 11), in which a pre-charged capacitor is discharged in the copper coil. This approach allowed us to obtain rising rates up to 660 T/s and fields up to 5 T. The applied magnetic field $B_a(t)$ was deduced from the current measured in the copper coil, and the magnetic field at the center of the two pellets $B_0(t)$ was measured with a Hall probe.

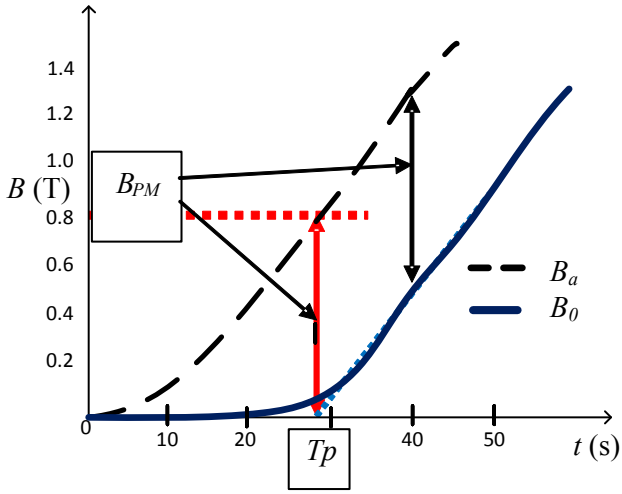

Fig. 12. Applied magnetic field B_a and measured magnetic field B_0 at the center of the pellet versus time for a low rising field rate. We also show $B_a(t)$-B_{PM} (blue dotted line).

In the experimental results (Fig. 12 and 13) the beginning of the rise of $B_0(t)$ does not exhibit the same waveform as that of $B_a(t)$. As it is confirmed later in the paper (part 3), this is due to the necessary space between the pellets to place the Hall probe. Therefore, the determination of the penetration time T_P is done as follows. A criterion is first chosen to clearly define T_P. Knowing T_P allows defining B_{PM}. In this case, we decided to define T_P using the measured magnetic field curve $B_0(t)$ at the center of the pellet. Firstly we consider that after complete penetration (for $T > T_P$) $B_a(t)$ and $B_0(t)$ are separated of B_{PM}. Secondly we modified $B_0(t)$ around T_P to be a copy of applied magnetic field $B_a(t)$, ($B_a(t) - B_{PM}$ shown in blue dotted line in Fig. 12 and 13). Thirdly we deduced T_P and B_{PM}. This is valid because after the complete penetration time T_p the difference between curves is nearly-constant and equals to B_{PM}, as clearly seen in Fig. 12 and Fig. 13.

In Fig. 14, which is the same figure as Fig. 13, but for a higher field and on a larger time scale, this approximation is less valid as we can see that the difference between $B_a(t)$ and $B_0(t)$ is not as constant in this case. The main reason for this difference between $B_a(t)$ and $B_0(t)$ at low and high fields is that J_C decreases with B. In fact, the difference is proportional to J_C.

Overall, the greater $B_a(t)$ is, the smaller the difference between $B_a(t)$ and $B_0(t)$ is. Despite this approximation, we chose this criterion for defining T_P in order to allow comparisons between the two rising rates (Fig. 12 and 13).

With the criterion chosen and for our two YBaCuO pellets (Fig. 9), the measured B_{PM} were: B_{PM1} = 1.0 T for the high rising field rate (V_{b1} = 660 T/s), and B_{PM2} = 0.8 T for the low rising rate (V_{b2} = 0.033 T/s) (Fig.12 and 13).

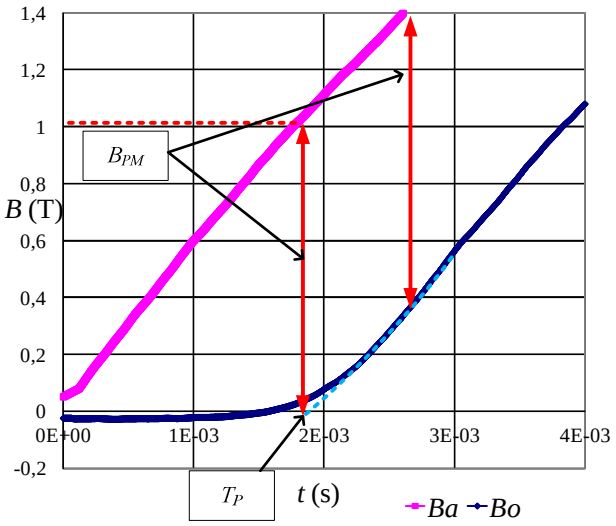

Fig. 13. Applied magnetic field B_a and measured magnetic field at the (blue dotted line).

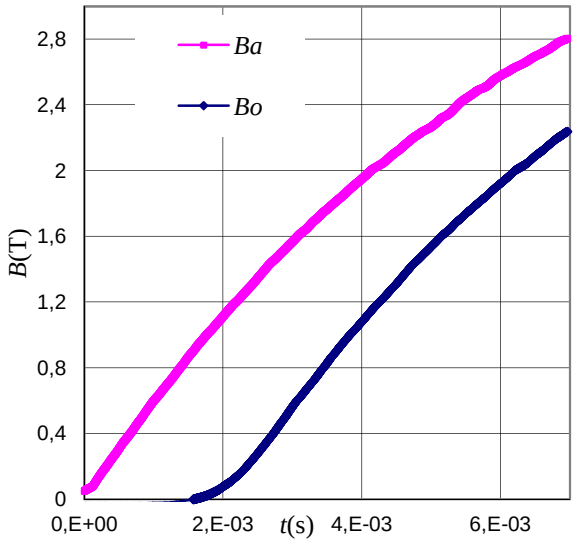

Fig. 14. Applied magnetic field B_a and measured magnetic field at the center of the pellet B_0 for a high rising field rate.

5. *n*-value and J_C determination method

The determination of the *n*-value and J_C of a pellet was done as follows. We first identify the two measured values of B_{PM} as explained above, corresponding to two different values of V_b. From these values, the n-value can be deduced with:

$$n = \frac{\alpha.\left(B_{PM2}.lnV_{b1} - B_{PM1}.lnV_{b2}\right)}{B_{PM1} - B_{PM2}} - \beta \qquad (11)$$

From this n-value, and with B_{P1}, V_{b1} and (10), we can deduce the value of B_{PB}. Finally, from (2) and the geometric parameters *R* and *L*, we determine J_C. To correctly connect simulation and experimental results, the influence of Hall probe thickness e must be taken into account. Fig. 15 presents simulations made with two pellets and different spacings (e = 0.5 and 1 mm), typical of Hall probe thicknesses. We then compared those results with those of a single pellet without hall probe (e = 0 mm).

Fig. 15 shows that T_P and B_{PM} increase with e. This is due to the shape of the current density distribution near the center of the pellets (see Fig.16). Without the Hall probe, the region without current has a circular shape, as shown in Fig. 3. With the Hall probe, this zero current region becomes two regions with ovoid-like shape, corresponding to a quicker current density penetration than without the probe. Although the probe thickness should be reduced as much as possible, numerical simulations allow correcting the measured value B_{PM} in order to obtain a relatively good value of B_P.

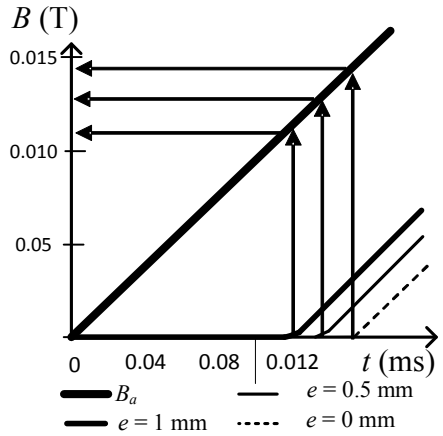

Fig. 15. B_a(t) and B_0(t) for different Hall probe thicknesses e.

From our experiments, we find V_{b1} = 660T/s, B_{PM1} = 1.0 T, V_{b2} = 0.033 T/s and B_{PM2} = 0.8 T. After taking into account the probe thickness e = 1.0 mm, we find the corrected values of complete penetration magnetic are B_{P1} = 1.3 T, and B_{P2} = 1.0 T. With these values, we find a n-value of 50, which is possible for monocrystaline YBCO pellets at 77 K. The value of B_{PB} calculated with (11) and n = 50 is 1.1 T and the value of J_C deduced is 110 A/mm². Once again, this value is consistent with commonly used YBCO pellets at 77 K

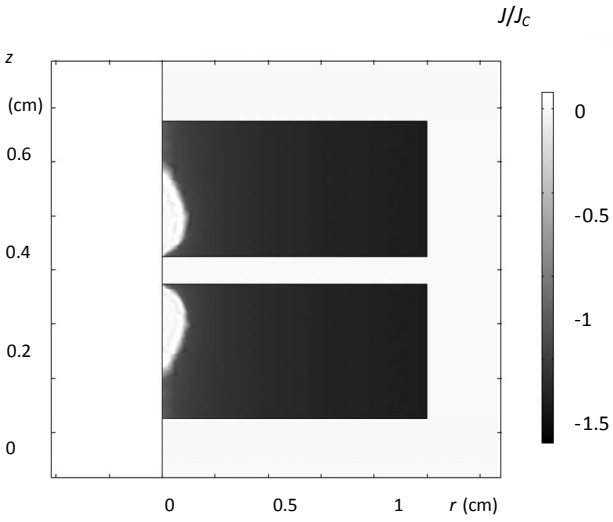

Fig. 16 Current density distribution in superconducting pellet for e = 1 mm.

6. Conclusion.

In this paper, we present a new experimental approach to identify the J_c and *n*-value of YBCO pellets through a simple magnetization experiment correlated with a numerical simulation. The principle relies on that we can identify the two parameters through two measurements at different applied magnetic field rising rate V_b. Indeed, by

deducing from measurements the complete penetration magnetic field B_P of a high temperature superconducting cylinder under two different V_b, we can uniquely determine J_c and n using a simple linear relationship between B_P, V_b and n-value, whose parameters are determined by simulation a priori. This new relationship is likely to be very useful in the future for application sizing. In practice, the measurement of B_{PM} is made with two HTS pellets at once, in order to insert a Hall probe and be able to deduce the required values of B_p. Since the simulation is used to establish the linear model parameters, it is quite easy to take the sensor thickness into account and still find an accurate solution. Further validation of the method should be realized on various samples and in more experimental conditions.

Acknowledgments

The authors thank Region Lorraine for financial support.

References

[1] A. Rezzoug, J. Leveque, B. Douine, S. Mezani, "Superconducting machines", in *Non-conventional electrical machines*, Wiley, 2012, pp. 191-255.

[2] P. Masson, J Leveque, D Netter, A. Rezzoug, "Experimental study of a new kind of superconducting inductor", *IEEE Trans. on Appl. Supercond*, Vol. 13(2), pp. 2239-2242, 2003

[3] E. Ailam, D. Netter, J. Leveque, B. Douine, P. Masson, A. Rezzoug, "Design and Testing of a Superconducting Rotating Machine", *IEEE Trans. on Appl. Supercond*., vol.17(1), pp.27-33, 2007.

[4] R. Moulin, J. Leveque, L. Durantay , B. Douine, D. Netter, A. Rezzoug, "Superconducting Multi-Stacks Inductor for Synchronous Motors Using the Diamagnetism Property of Bulk Material," *IEEE Trans. on Industrial Electronics*, vol. 57, no. 1, pp. 146-153, 2010

[5] P. Masson, M. Breschi, P. Tixador, C.A. Luongo, "Design of HTS axial flux motor aircraft propulsion", *IEEE Trans. on Appl. Supercond*, Vol. 17(2), pp. 1533-1536, 2007

[6] S. Ishmael, P. J. Masson, R. Meinke, C. Goodzeit, R. Sullivan, "Flux Pump Excited Double-Helix Rotor for Use in Synchronous Machines", *IEEE Trans. on Appl. Supercond.*, Vol. 18(2), pp693-696, 2008

[7] W. Xian, Yan Y., Yuan W, Pei R.,T.A. Coombs "Pulsed field magnetization of a HTS motor", *IEEE Trans. App. Supercond*., Vol. 21(3), pp. 1171-1174, 2011

[8] M. Miki, B. Felder, K. Tsuzuki, Y. Xu, Z. Deng, M. Izumi, H. Hayakawa, M. Morita, H. Teshima, "Materials processing and machine applications of bulk HTS", *Supercond. Sci. Tech*., vol.23, 124001, 2010

[9] D. Zhou, M. Izumi, M. Miki, B. Felder, T. Ida, M. Kitano, "An overview of rotating machine systems with high-temperature bulk superconductors", *Supercond. Sci. Tech.*, vol.25, 103001, 2012

[10] T.A. Coombs "A Finite Element Model of Magnetization of Superconducting Bulks Using a Solid-State Flux Pump", *IEEE Trans. App. Supercond*., Vol. 21(6), pp. 3581-3586, 2011.

[11] A. Sanchez, C. Navau, "Critical current density from magnetization loops of finite high-TC superconductors," *Supercond. Sci. Tech*., vol.14, pp.444-447, 2001.

[12] T.A. Coombs, A. M. Campbell, A. Murphy, M. Emmens, "A fast algorithm calculating the critical state in superconductor," *COMPEL*, vol. 20, n°1, pp. 240-252, 2001.

[13] B. Douine, F. Sirois, J. Leveque, K. Berger, C.H. Bonnard, T.C. Hoang, S. Mezani, "A New Direct Magnetic Method for Determining Jc in Bulk Superconductors From Magnetic Field Diffusion Measurements," *IEEE Trans. on Appl. Supercond*., vol. 22 (3), 9001604, 2012.

[14] B. Douine, J. Leveque, S. Mezani, "J_C(B) determination method with the help of the virgin magnetization curve of a superconducting cylinder," *IEEE Trans. on Appl. Supercond*., vol. 20 (2), pp.82-86, 2010.

[15] C. P. Bean, "Magnetization of high-field superconductors," *Rev. Mod. Phys.*, pp.31-39, Jan. 1964.

[16] D.X. Chen, A. Sanchez, C. Navau, Y.H. Shi, D.A. Cardwell, "Critical current density of melt-grown single YBaCuO disks determined by ac susceptibility measurements," *Supercond. Sci. Tech*., vol. n°21, 085013, 6 pp., 2008.

[17] I. Mayergoys, "Nonlinear diffusion of electromagnetic fields", *Academic press*, 407 p., 1998

[18] A. Kameni, D. Netter, S. Mezani, B. Douine, J. Leveque,"Scaling Solution and n Dependence of the Eddy-Current Distribution in a Flat Superconductor", *IEEE Trans. on Appl. Supercond*., vol. 20 (4), pp. 2248-2254, 2010.

[19] P. Vanderbemden, "Determination of critical current in bulk high temperature superconductors by magnetic flux profile measuring methods", Ph. D Thesis, University of Liège, 193 p, 1999.

[20] A. Kameni-Ntichi, J. Leveque, B. Douine, S. Mezani, D. Netter, "Influence of speed variation of a transverse magnetic field on a magnetization of HTS cylinder," *IEEE Trans. on Appl. Supercond*., vol.21, n°4, august 2011.

[21] D.X. Chen, E. Pardo, "Power law E(J) characteristic converted from field-amplitude and frequency dependent ac susceptibility in superconductors," *Applied physics letters*, vol. n°88, 222505, 3 pp., 2006.

[22] R. B. Goldfarb, M. Lelental, C.A. Thompson, "Alternating field susceptometry and magnetic susceptibility of superconductors," in *Magnetic susceptibility of superconductors and other spin systems* Plenum Press, pp. 49-80, 1992.

[23] E. Durand, *Electrostatique et magnetostatique*, Masson, 774 p., 1953.

[24] A. Forkl, "Magnetic flux distribution in single crystalline, ceramic and thin film high-Tc-superconductors," *Physica Scripta*, T49, pp. 148-158, 1993.

[25] E.H. Brandt, "Superconductor disks and cylinder in an axial magnetic field, field penetration and magnetization curves," *Physical Review B*, vol. 58, n°10, pp. 6506-6522, 1998.

[26] H. T. Coffey, "Distribution of magnetic fields and currents in type II superconductors," *Cryogenics*, vol. 7, pp.73-77, 1967.

[27] D.J. Frankel, "Critical state model for the determination of critical currents in disk shaped superconductors," *J. Appl. Phys*., vol.50, n° 8, pp. 5402-5407, 1979.

[28] K. Berger, J. Leveque, D. Netter, B. Douine, A. Rezzoug, Influence of temperature and/or field dependence of the E-J power law on trapped magnetic field in bulk YBaCuO., *IEEE Trans. on Appl. Supercond.*, 17(2), pp.3028-3031, june 2007.

[29] F. Sirois, F. Grilli, "Numerical considerations about using FEM to compute AC losses in HTS," *IEEE Trans. on Appl. Supercond*., vol. 18, n°3, 2008

[30] R. Brambilla, F. Grilli, and L. Martini, "Development of an edge-element model for AC loss computation of high-temperature superconductors," *Supercond. Sci. Tech*., vol. 20, no. 1, pp. 16–24, 2007.

[31] B. Dutoit, J. Duron, S. Stavrev, and F. Grilli, "Dynamic Field Mapping for Obtaining the Current Distribution in High-Temperature Superconducting Tapes," *IEEE Trans. on Appl. Supercond.*, vol. 15, n°2, 2005.

[32] J. Fagnard, M. Dirickx, M. Aussloss, G. Lousberg, P. Vanderbemden, B. Vanderheyden, "Magnetic shielding properties of high-Tc superconducting hollow cylinders: model combining experimental data for axial and transverse magnetic field configurations," *Superconductor science and technology*, vol.22, 10, 105002, 2009.

[33] P. Laurent, J. Fagnard, N. Babu, D.A. Cardwell, B. Vanderheyden, P. Vanderbemden, "Self heating of bulk HTS of finite height subjected to a large alternating magnetic field," *Supercond. Sci. Tech.*, vol.23, 12, 124004, 2010.

Bruno Douine was born in Montereau, France, in 1966. He received his Ph. D. degree in electrical engineering from University of Nancy, France, in 2001.

He is currently Full Professor of the University of Lorraine. As member of the Groupe de Recherche en Electrotechnique et Electronique de Nancy, his main subjects of research concern characterization and modeling of superconducting material and applied superconductivity in electrical

engineering. He is a Regular Reviewer for several international journals and conferences.

Charles-Henri Bonnard (S'14) was born in Épinal, France, in 1985. He received the M.Sc. Degree in electrical engineering from the École Polytechnique de Montréal, Montréal, QC, Canada, in 2012.
He is currently working toward the Ph.D. degree in electrical engineering at the same university. His main research interests include modeling, simulation and integration of superconducting apparatus in power systems.

Frédéric Sirois (S'96–M'05–SM'07) received the B.Eng. degree in electrical engineering from Université de Sherbrooke, Sherbrooke, QC, Canada, in 1997, and the Ph.D. degree from École Polytechnique de Montréal, Montréal, QC, Canada, in 2003. From 1998 to 2002, he was affiliated as a Ph.D. Scholar with Hydro-Québec's Research Institute (IREQ). From 2003 to 2005, he was a Research Engineer with IREQ. In 2005, he joined École Polytechnique de Montréal where he is now a Full Professor. He is also a Regular Reviewer for several international journals and conferences. His main research interests include modeling and design tools for magnetic and superconducting devices, integration studies of superconducting equipment in power systems, and planning of power systems.

Kevin Berger received the Ph.D. degree in electrical engineering from the Université Henri Poincaré, Nancy, France, in 2006. From 2006 to 2008, he was with the Grenoble Electrical Engineering Laboratory (G2Elab) and the Néel Institut, Grenoble, France, as a Postdoctoral Researcher in order to work on superconductor modeling using FLUX software and an HTS conduction-cooled SMES. Since 2010, he has been an Assistant Professor with the University of Lorraine, Nancy. His research interests deal with the design and modeling of superconducting devices such as cryomagnets while taking into account coupled magneto-thermal behavior. His research topics also include electrical characterization of superconducting material and ac loss measurements.

Abelin Kameni was born in Yaounde, Cameroon, in 1979. He is an Engineer from "Ecole D'Ingénieurs en Modélisation Mathématique et Mécanique (MATMECA)" in 2004. He received the M.Sc. degree in Mathematical modeling from University of Bordeaux in 2005. In 2009 he earned a PhD in Electrical Engineering of Université Henri Poincarré from Nancy and joined the Group of Electrical Engineering of Paris (GeePS) in 2010 as Assistant Professor. His research interests concern numerical methods applied to electromagnetic problems.

Jean Lévêque was born in Angers, France, in 1963. He received his Ph. D. in electrical engineering from University of Grenoble, France, in 1993.
He is currently Professor at the University of Nancy. As member of the Groupe de Recherche en Electrotechnique et Electronique de Nancy, his main subjects of research concern characterization and modelization of superconducting material and applications.